



Non-Arrhenian Temperature-Dependent Viscosity of Alkali(ne) Carbonate Melts at Mantle Pressures

Xenia Ritter¹, Bertrand Guillot², Nicolas Sator², Elsa Desmaele², Malcolm Massuyeau¹ and Carmen Sanchez-Valle^{1*}

¹Institut für Mineralogie, Westfälische Wilhelms-Universität Münster, Münster, Germany, ²Laboratoire de Physique Théorique de la Matière Condensée, CNRS, Sorbonne Université, Paris, France

OPEN ACCESS

Edited by:

Mainak Mookherjee,
Florida State University, United States

Reviewed by:

Zhicheng Jing,
Southern University of Science and
Technology, China
Aaron Wolf,
University of Michigan, United States

*Correspondence:

Carmen Sanchez-Valle
sanchezm@uni-muenster.de

Specialty section:

This article was submitted to
Earth and Planetary Materials,
a section of the journal
Frontiers in Earth Science

Received: 01 March 2021

Accepted: 22 September 2021

Published: 15 October 2021

Citation:

Ritter X, Guillot B, Sator N,
Desmaele E, Massuyeau M and
Sanchez-Valle C (2021) Non-Arrhenian
Temperature-Dependent Viscosity of
Alkali(ne) Carbonate Melts at
Mantle Pressures.
Front. Earth Sci. 9:674770.
doi: 10.3389/feart.2021.674770

The viscosity of carbonate melts is a fundamental parameter to constrain their migration and ascent rates through the mantle and ultimately, their role as carbon conveyors within the deep carbon cycle. Yet, data on the viscosity of carbonate melts have remained scarce due to experimental limitations and the lack of appropriate theoretical descriptions for molten carbonates. Here, we report the viscosity of $K_2Mg(CO_3)_2$ and $K_2Ca(CO_3)_2$ melts up to 13 GPa and 2,000 K by means of classical molecular dynamics (MD) simulations using optimized force fields and provide first evidence for non-Arrhenian temperature-dependent viscosity of molten carbonates at mantle pressures. The viscosity of $K_2Mg(CO_3)_2$ and $K_2Ca(CO_3)_2$ melts ranges respectively between 0.0056–0.0875 Pa s and 0.0046–0.0650 Pa s in the investigated pressure-temperature interval. Alkali(ne) carbonate melts, i.e. mixed alkali and alkaline earth carbonate melts - $K_2Mg(CO_3)_2$ and $K_2Ca(CO_3)_2$ - display higher viscosity than alkaline earth carbonate melts - $CaCO_3$ and $MgCO_3$ - at similar conditions, possibly reflecting the change in charge distribution upon addition of potassium. The non-Arrhenian temperature-dependence of the viscosity is accurately described by the Vogel-Fulcher-Tammann model with activation energies E_a for viscous flow that decrease with temperature at all investigated pressures, e.g. from ~100 kJ/mol to ~30 kJ/mol between 1,300 and 2,000 K at 3 GPa. Pressure is found to have a much more moderate effect on the viscosity of alkali(ne) carbonate melts, with activation volumes V_a that decrease from 4.5 to 1.9 cm³/mol between 1,300 and 2,000 K. The non-Arrhenian temperature-viscosity relationship reported here could be exhibited by other carbonate melt compositions as observed for a broad range of silicate melt compositions and it should be thus considered when modeling the mobility of carbonate melts in the upper mantle.

Keywords: carbonate melts, viscosity, classical MD simulations, non-arrhenian, upper mantle

INTRODUCTION

Despite the rare occurrence of carbonate-rich volcanism in the present-day Earth (Woolley and Kjarsgaard, 2008; Jones et al., 2013), carbonate melts produced by incipient melting of carbonated lithologies play a critical role in subsurface magmatic processes and they are major phases for the storage and transport of carbon in the upper mantle (Dasgupta and Hirschmann, 2010; Dasgupta, 2013; Stagno, 2019). The percolation of carbonate-rich melts through the mantle, even at melt fractions as low as < 0.1 vol% (Gaillard et al., 2008; Massuyeau et al., 2021), has a large impact on the geochemical and geodynamic evolution of the Earth's interior. Because of their excellent wetting properties, low density and low viscosity (e.g. Minarik and Watson, 1995; Dobson et al., 1996; Hammouda and Laporte, 2000; Kono et al., 2014; Ritter et al., 2020), carbonate melts are regarded as efficient metasomatic agents involved in the redistribution of incompatible trace elements and volatiles in the mantle (Green and Wallace, 1988; Yaxley et al., 1991; Rudnick et al., 1993; Dixon et al., 2008; Kiseeva et al., 2012; Poli, 2015; Keller et al., 2017), as well as in the generation of diamond-forming kimberlitic magmatism (Dalton and Presnall, 1998; Korsakov and Hermann, 2006; Russell et al., 2012; Sparks, 2013; Sun and Dasgupta, 2019). Besides, carbonate-rich melts are often proposed as an explanation for the low velocity zones (Dasgupta and Hirschmann, 2010; Fischer et al., 2010; Gardés et al., 2020) and electrical anomalies (Gaillard et al., 2008; Naif et al., 2013; Sifré et al., 2014; Massuyeau et al., 2021) observed at the Lithosphere-Asthenosphere-Boundary (LAB) beneath oceanic ridges and continents.

Although the chemistry and reactivity of carbonate-rich melts has been extensively investigated over the past decades (e.g., Wallace and Green, 1988; Veksler et al., 1998; Yaxley and Brey, 2004; Gudfinnsson and Presnall, 2005; Hammouda and

Keshav, 2015 and references therein; Gervasoni et al., 2017), their physical properties (e.g. density and viscosity) remain poorly constrained to date despite their control on melt mobility through the mantle (**Table 1**). Particularly, the viscosity of melts governs the migration rates and the efficiency of melt transport across the mantle, hence affecting the carbon fluxes at depth and towards the surface (Keller et al., 2017). Data scarcity for mantle carbonate melts at relevant pressure-temperature conditions reflects the experimental challenges associated with direct viscosity measurements due to their high reactivity (Treiman and Schedl, 1983; Treiman, 1995), and the limitations of theoretical formalisms to predict the properties of complex chemical systems (Vuilleumier et al., 2014; Wilding et al., 2016; Wilson et al., 2018; Desmaele et al., 2019a, 2019b; Hurt and Wolf, 2019). Experimental studies of carbonate melt viscosity have thus been performed mostly at room pressure for endmember alkali (Li, K, Na) carbonate melts as well as their binary mixtures (e.g., Janz, 1988; Sato et al., 1999; Di Genova et al., 2016), with only three studies reporting carbonate melt viscosities at high pressure to date (Dobson et al., 1996; Kono et al., 2014; Stagno et al., 2018). Pioneering measurements by Dobson et al. (1996) using the falling sphere technique coupled with synchrotron X-ray imaging determined the viscosity of $K_2Mg(CO_3)_2$ and $K_2Ca(CO_3)_2$ melts up to 5.5 GPa. Reported viscosities for those compositions are however ca. one order of magnitude larger than more recent results for $CaCO_3$, $CaMg(CO_3)_2$ and Na_2CO_3 melts obtained by using an ultrafast X-ray imaging technique with improved accuracy on the viscosity determination (Kono et al., 2014; Stagno et al., 2018). Interestingly, these later studies report comparable viscosities for all investigated compositions and negligible pressure effects on the viscosity that are difficult to reconcile with computational studies (Desmaele et al., 2019a; 2019b). The scarcity of currently available data thus precludes the identification of pressure,

TABLE 1 | Compilation of available high pressure viscosity data for alkali(ne) carbonate melts from experiments and classical/*ab-initio* MD simulations.

Melt composition	Pressure [GPa]	Temperature [K]	Method	Reference
$K_2Mg(CO_3)_2$ (KM)	3, 5.5	1,073–1,473	Synchrotron shadowgraph + Falling sphere	Dobson et al. (1996)
	3	1,247–1,687	Classical MD	Desmaele et al. (2019b)
	10^{-4} –13	1,200–2,000	Classical MD	This study
$K_2Ca(CO_3)_2$ (KC)	2.5, 4	1,223–1,423	Synchrotron shadowgraph + Falling sphere	Dobson et al. (1996)
	10^{-4} , 2.5, 3	1,094–1,584	Classical MD	Desmaele et al. (2019b)
	10^{-4} –13	1,200–2,000	Classical MD	This study
K_2CO_3 (K)	4	1,773	Synchrotron shadowgraph + Falling sphere	Dobson et al. (1996)
	10^{-4} –15	1,100–2,073	Classical MD	Desmaele et al. (2019a) ^a
$CaCO_3$ (C)	0.9–6.2	1,653–2,063	Synchrotron + Falling sphere	Kono et al. (2014)
	10^{-4} –15	1,100–2,073	Classical MD	Desmaele et al. (2019b) ^a
	10^{-4} –15	1,623–3,273	Classical MD + Ab-initio MD	Vuilleumier et al. (2014) ^a
$MgCO_3$ (M)	10^{-4} –15	1,873–2,073	Classical MD	Desmaele et al. (2019b) ^a
$CaMg(CO_3)_2$ (CM)	3–5.3	1,683–1,783	Synchrotron + Falling sphere	Kono et al. (2014)
	10^{-4} –15	1,653–2,073	Classical MD	Desmaele et al. (2019b) ^a
Na_2CO_3	1.7–4.6	1,473–1,973	Synchrotron + Falling sphere	Stagno et al. (2018)
	10^{-4} –15	1,100–2,073	Classical MD	Desmaele et al. (2019a) ^a
25M75K	2	1,523	Synchrotron shadowgraph + Falling sphere	Dobson et al. (1996)

^aSelected P-T conditions, typically two temperature conditions per isobar.

temperature and compositional effects on the viscosity of carbonate melts and hence, the quantitative modelling of melt migration processes (**Table 1**).

In the past decades, computational methods have emerged as a powerful tool to probe the chemical structure and physical properties, including the viscosity, of molten systems at high pressure-temperature conditions difficult to access experimentally (e.g. Kubicki and Lasaga, 1988; Rustad et al., 1990; Tissen et al., 1994; Genge et al., 1995; Guillot and Sator, 2007a, 2007b, 2011; Vuilleumier et al., 2014; Corradini et al., 2016; Wilding et al., 2016, 2019; Li et al., 2017; Dufils et al., 2017, 2018; Wilson et al., 2018; Desmaele et al., 2019b, 2019a; Hurt and Wolf, 2019). Molecular dynamics (MD) simulations based on *ab initio* and/or classical approaches have thus significantly contributed to expand the available viscosity datasets for carbonate melts at relevant pressure-temperature conditions (**Table 1**). Nevertheless, the theoretical studies remain largely limited to simple endmember compositions due to the high computational cost of the *ab initio* calculations and the lack of appropriate force-fields to describe the atomic/ionic interactions in classical simulations of complex multicomponent carbonate melts (Genge et al., 1995; Vuilleumier et al., 2014; Li et al., 2017; Desmaele et al., 2019a, 2019b; Hurt and Wolf, 2019). Recently, Desmaele et al., (2019a) developed optimized classical force-fields for molten carbonates in the system $\text{Li}_2\text{CO}_3\text{-Na}_2\text{CO}_3\text{-K}_2\text{CO}_3\text{-MgCO}_3\text{-CaCO}_3$ based on experimental data and melt structures issued from *ab initio* simulations of molten CaCO_3 (Vuilleumier et al., 2014), MgCO_3 , $\text{CaMg}(\text{CO}_3)_2$ (Desmaele et al., 2019b), Na_2CO_3 and K_2CO_3 (Desmaele et al., 2019a). These force-fields accurately reproduce experimental data on the density (e.g. Liu and Lange, 2003; O'Leary et al., 2015), viscosity (e.g. Janz, 1988; Kono et al., 2014) and electrical conductivity (e.g. Gaillard et al., 2008; Kojima, 2009; Sifré et al., 2014) of simple and binary carbonate melts. These results open the possibility for studies of the viscosity of complex carbonate melts at pressure and temperature conditions previously unexplored (**Table 1**).

Here, classical molecular dynamics simulations using the optimized force-fields developed by Desmaele et al. (2019a) have been conducted to determine the viscosity of alkali(ne) melts, i.e. mixed alkali and alkaline-earth carbonate melts - $\text{K}_2\text{Mg}(\text{CO}_3)_2$ and $\text{K}_2\text{Ca}(\text{CO}_3)_2$ - up to 13 GPa between 1,000 and 2,000 K. These compositions mimic incipient melts of subducted continental potassium rich lithologies at high pressure (8–13 GPa; Grassi and Schmidt, 2011b, 2011a; Kiseeva et al., 2013) and allow a direct comparison of the results with previous high pressure experimental studies (Dobson et al., 1996). The results constrain pressure and temperature effects on the viscosity of alkali(ne) carbonate melts and reveal non-Arrhenian temperature-viscosity relations that could not be anticipated from the data available to date.

MATERIALS AND METHODS

A total of 106 classical MD simulations were performed to determine the viscosity of $\text{K}_2\text{Mg}(\text{CO}_3)_2$ and $\text{K}_2\text{Ca}(\text{CO}_3)_2$ (hereafter referred to as KM and KC, respectively) melts

from room pressure to 13 GPa and 1,000–2,000 K, with 1–3 GPa and 100 K increments. The MD simulations were conducted with the DL_POLY 2.0 code (Smith and Forester, 1996) in the microcanonical (NVE) ensemble, where the number of atoms (N), the volume (V) and the total energy (E) are fixed. The pressure (P) and temperature (T) conditions at equilibrium were determined in isothermal-isobaric (NPT ensemble) runs using a Nosé-Hoover thermostat. The thermodynamic parameters, P, T and E_{Pot} are calculated from block averages of 500 k time steps after the system has reached equilibrium (**Figure 1**). The system was composed of $N = 2002$ atoms in a cubic box with periodic boundary conditions in 3D (**Figure 1**) as described in Desmaele et al. (2019b). The interionic interactions were described using empirical force fields recently developed for alkali and alkaline carbonate melts that take into account both the long-range Coulomb interactions and the short-range repulsion-dispersion interactions (Desmaele et al., 2019a). The force field is decomposed as a sum of pair potentials for the intramolecular (i.e. interactions within a carbonate CO_3^{2-} molecule) and intermolecular (i.e. between all ions) contributions, where the carbonate ion is featured as flexible and nondissociative (for further details see Desmaele et al., 2019a; 2019b). The interaction parameters employed in the simulations are those reported in Desmaele et al. (2019a, 2019b). The equations of motion for atoms were solved using the Verlet algorithm with a time step of 1 fs (10^{-15} s) and simulation runs lasted for 10^7 steps (i.e. 10–20 ns). The run duration is thus sufficiently long compared to the characteristic time scale for viscous relaxation τ in carbonate melts, i.e. few ps to tens of ps as given by the Maxwell relation $\tau = \eta/G_\infty$, where the shear modulus at infinite high frequencies G_∞ is $\sim 10^{10}$ Pa (Dingwell and Webb, 1999) to achieve convergence of the simulations even at the lowest temperatures investigated here (Desmaele et al., 2019b). The convergence is confirmed by the attainment of a viscosity plateau region in the time-dependence of the simulated viscosity at all P-T conditions and thus ensures the robustness of the reported viscosity data (**Figure 1D** and **Supplementary Figure S1**).

The shear viscosity of carbonate melts was then calculated by intergrating the auto-correlation function of the off-diagonal elements of the stress tensor $S(t)$ using the Green-Kubo equation (Boon and Yip, 1980; Hess, 2002; Vuilleumier et al., 2014):

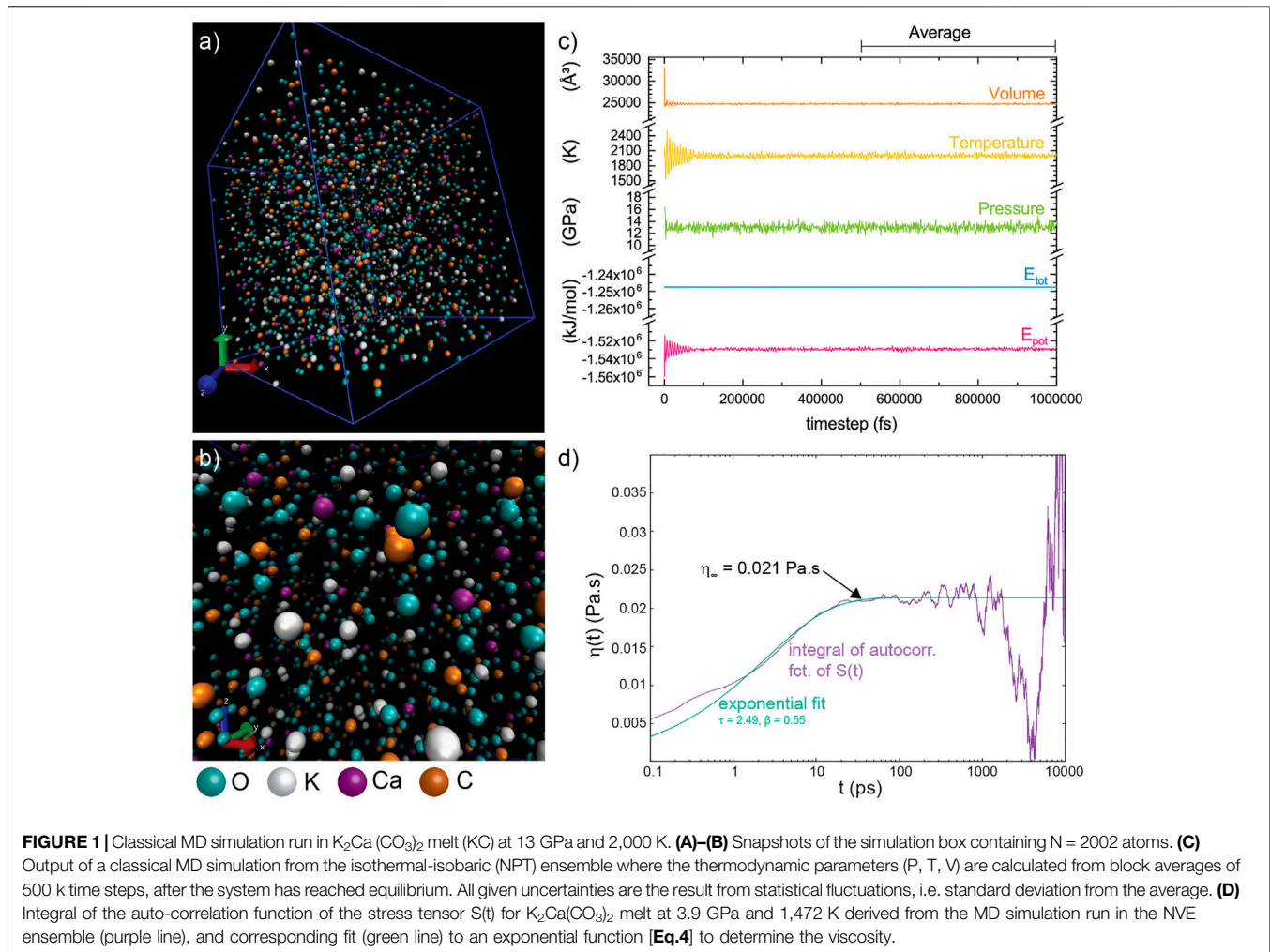
$$\eta = \frac{1}{k_B TV} \int_0^\infty S(t) dt \quad (1)$$

where k_B is the Boltzmann's constant and $S(t)$ is described as:

$$S(t) = \sum_{\alpha \neq \beta} \langle P_{\alpha\beta}(t) \cdot P_{\alpha\beta}(0) \rangle \quad (\alpha, \beta = x, y, z) \quad (2)$$

$$P_{\alpha\beta} = \sum_{i=1}^N m_i v_i^\alpha v_i^\beta + \sum_{i=1}^N \sum_{j>i}^N F_{ij}^\alpha r_{ij}^\beta \quad (3)$$

where m_i is the mass of the ion i , v_i^α is the component α of its velocity, r_{ij}^β and v_i^β are the component β of the distance between



ions i and j , and the velocity of the atom i , respectively, and F_{ij}^α is the component α of the force acting between ions i and j . The brackets refer to an average over the trajectories of all the ions in the simulation cell. Subsequently, the viscosity is derived by fitting the integral of the auto-correlation function of the stress tensor by an exponential function (Figure 1D):

$$\eta(t) = \eta_\infty \left(1 - e^{\left(-\frac{t}{\tau}\right)^\beta} \right) \quad (4)$$

where η_∞ is the desired viscosity, τ is the viscous relaxation time, and β is the stretching factor, which ranges between 0 (ultra-low viscosity melts) and 1 (highly viscous melts). A least-square minimization fit is performed in the short time shift region, where the statistics on the integrated auto-correlation function of $S(t)$ is excellent (e.g. < 100 ps in Figure 1D), to retrieve the viscosity plateau independently of the fluctuations at long time shifts that could bias the results (Supplementary Figure.S1).

The accuracy of the auto-correlation function strongly depends on the number of time steps. Therefore, simulation runs were extended to 20 ns to keep the statistical uncertainties on the viscosity data around $\pm 15\%$ up to 1,700–1,800 K as estimated

from the quality of the fit to the integrated auto-correlation function of the stress tensor $S(t)$ (Figure 1D). Uncertainties further increase with temperature due to the larger fluctuations in temperature (and pressure), particularly during large simulation runs (Zhang et al., 2015), which hamper the unambiguous identification of the plateau region of the Green-Kubo integral to extract the viscosity (Figure 1D). We conservatively estimate that total uncertainties can reach ca. $\pm 40\%$ at 2,000 K, the highest temperature of this study, although the overall precision is much better and typically yields viscosities within 10–15%. Statistical fluctuations on pressure and temperature were typically $\Delta P = \pm 0.5$ GPa and $\Delta T/T = \pm 1\%$, respectively.

The stability of the melt phase at all investigate pressure-temperature conditions was verified by monitoring the atomic diffusion coefficients that, even at the highest pressures, display characteristic values for molten systems with e.g. $D_{CO_3^{2-}} \sim 1 \times 10^{-9}$ to $7 \times 10^{-9} \text{ m}^2/\text{s}$ (Desmaele et al., 2019a). Furthermore, the investigated conditions up to 6 GPa fall above the experimental liquidus reported for the K_2CO_3 - $MgCO_3$ and K_2CO_3 - $CaCO_3$ systems (Ragone et al., 1966; Cooper et al., 1975; Shatskiy et al., 2015).

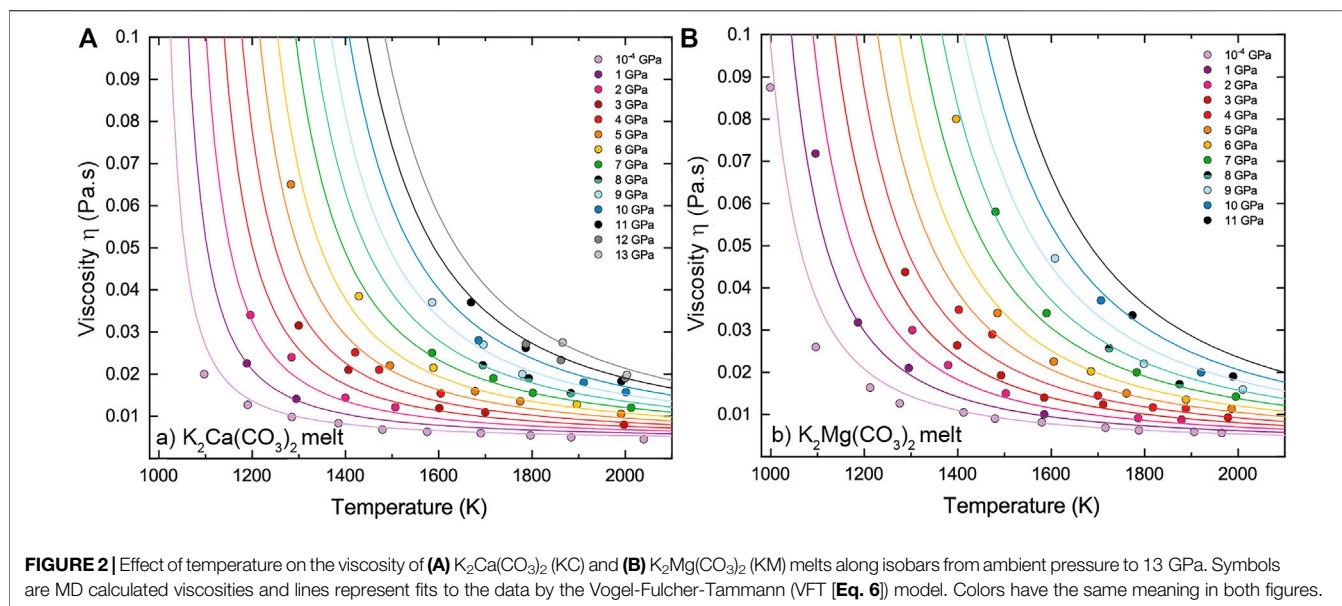
TABLE 2 | Viscosities of $K_2Mg(CO_3)_2$ and $K_2Ca(CO_3)_2$ melts computed in the NVE ensemble as a function of pressure and temperature conditions. Uncertainty for pressure and temperature are ± 0.5 GPa and 1%, respectively. Uncertainties in viscosity are typically $\pm 15\%$ up to 1,800 K and ca. $\pm 40\%$ at higher temperatures.

$K_2Mg(CO_3)_2$ (KM) melt			$K_2Ca(CO_3)_2$ (KC) melt		
Pressure	Temperature	Viscosity η	Pressure	Temperature	Viscosity η
GPa	K	Pa s	GPa	K	Pa s
10^{-4}	999	0.088	10^{-4}	1,097	0.020
10^{-4}	1,096	0.026	10^{-4}	1,190	0.013
1.0	1,095	0.072	1.0	1,188	0.023
10^{-4}	1,212	0.016	2.0	1,196	0.034
1.0	1,186	0.032	10^{-4}	1,285	0.0098
10^{-4}	1,275	0.013	1.0	1,294	0.014
1.0	1,295	0.021	1.9	1,284	0.024
2.0	1,302	0.030	3.0	1,300	0.032
3.0	1,287	0.044	4.9	1,282	0.065
10^{-4}	1,412	0.010	10^{-4}	1,385	0.0083
2.0	1,379	0.022	2.0	1,400	0.014
3.0	1,398	0.026	3.0	1,406	0.021
4.0	1,402	0.035	4.1	1,420	0.025
6.0	1,396	0.080	6.1	1,429	0.039
10^{-4}	1,480	0.0090	10^{-4}	1,479	0.0068
2.0	1,502	0.015	2.0	1,507	0.012
3.0	1,492	0.0193	3.9	1,472	0.021
3.9	1,473	0.0290	5.0	1,495	0.022
4.9	1,485	0.0340	10^{-4}	1,575	0.0063
6.9	1,481	0.0580	3.0	1,601	0.012
10^{-4}	1,580	0.0081	4.0	1,604	0.015
1.0	1,585	0.010	6.0	1,588	0.022
3.0	1,585	0.014	7.0	1,585	0.025
5.0	1,606	0.023	8.9	1,586	0.037
7.0	1,590	0.034	10^{-4}	1,690	0.0060
9.1	1,608	0.047	3.0	1,699	0.011
10^{-4}	1,716	0.0069	4.9	1,677	0.016
3.0	1,711	0.012	7.0	1,717	0.019
4.0	1,700	0.015	8.0	1,695	0.022
5.9	1,685	0.020	9.0	1,695	0.027
8.1	1,724	0.026	9.9	1,685	0.028
10.0	1706	0.037	10.9	1,669	0.037
10^{-4}	1,788	0.0062	10^{-4}	1,796	0.0055
2.0	1,786	0.0091	4.9	1,775	0.014
4.0	1,818	0.012	7.0	1,802	0.016
4.9	1,761	0.015	8.0	1,793	0.019
6.9	1,783	0.020	8.9	1,779	0.020
9.0	1,799	0.022	10.9	1,786	0.026
10.9	1,774	0.034	11.9	1,787	0.027
10^{-4}	1,906	0.0059	10^{-4}	1,884	0.0050
2.0	1,879	0.0088	6.0	1,896	0.013
4.0	1,888	0.011	8.0	1,883	0.016
6.0	1,889	0.014	10.0	1,911	0.018
7.9	1,875	0.017	11.9	1,862	0.023
10.1	1,921	0.020	12.9	1,865	0.028
11.9	1,874	0.029	10^{-4}	2,040	0.0046
10^{-4}	1,965	0.0056	3.0	1,997	0.0080
3.0	1,979	0.0093	5.0	1,991	0.0105
5.0	1,986	0.011	7.0	2,012	0.012
7.0	1,995	0.014	10.0	2,001	0.016
9.0	2,010	0.016	11.0	1,991	0.018
11.0	1,989	0.019	12.0	2,000	0.019
13.0	1,995	0.022	13.0	2,003	0.020

RESULTS

The simulation conditions and the viscosity results are summarized in **Table 2**. The viscosity of KM and KC melts

ranges respectively between 0.0056–0.0875 Pa s and 0.0046–0.0650 Pa s in the investigated pressure-temperature intervals. **Figures 2, 3** display the temperature and pressure dependence of the viscosity of KM and KC melts at the



investigated conditions. The viscosity of both melts follows a similar trend: it decreases with increasing temperature at constant pressure and increases linearly upon compression along an isotherm. Temperature appears as the primary control parameter on the viscosity of alkali(ne) carbonate melts whereas the effect of pressure is generally lower, although it is enhanced as temperature decreases (**Figure 3**). An interesting observation from the present results is that the viscosity of KM and KC melts only decreases linearly with temperature over a narrow (high) temperature interval (i.e. Arrhenian behavior), while a notable curvature in the $\log \eta$ vs $1/T$ data is apparent over the investigated temperature range at different pressures (**Figure 3**), thus indicating non-Arrhenian (i.e. fragile behavior, Angell, 1995) behavior. Yet, this behavior appears to become less pronounced as pressure increases, even though the temperature span of the data is more limited above 9 GPa (**Figure 3**). The non-Arrhenian evolution of the viscosity implies a temperature-dependent activation energy E_a of viscous flow (**Figure 4**) that may reflect changes in atomic/molecular-scale interactions and configuration in the melt (e.g. clustering) with temperature as discussed below (Glasstone et al., 1941). To the best of our knowledge, this is the first observation of non-Arrhenian temperature-dependent viscosity in carbonate melts at high pressure, a feature that could not be anticipated from the limited P-T range covered by previous studies (**Table 1**).

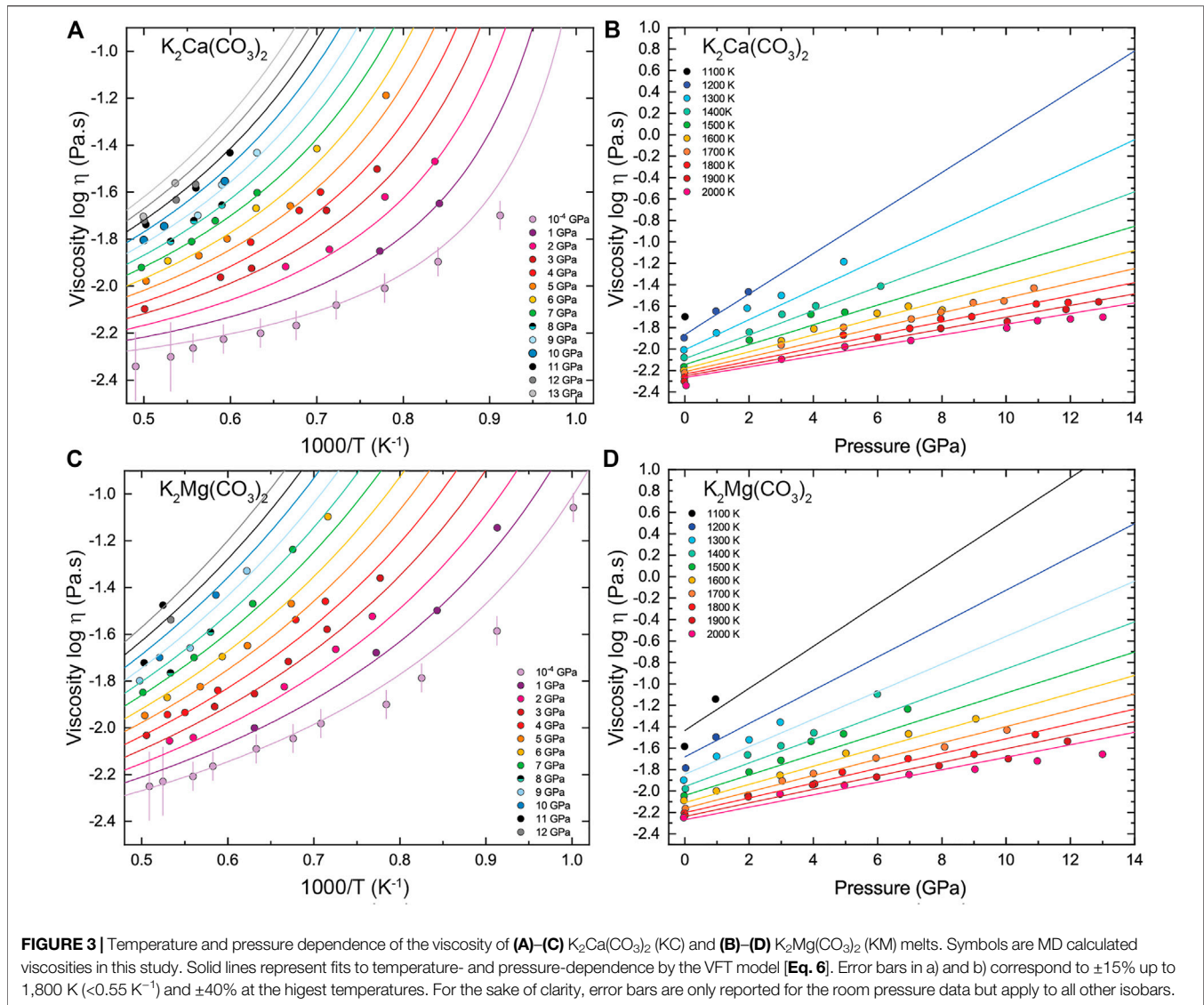
DISCUSSION

Effect of Temperature and Pressure on the Viscosity of Alkali(ne) Carbonate Melts

The viscosities of KM and KC melts reported here typically agree within errors with previous simulations by Desmaele et al.

(2019b), with the exception of the highest temperature data where differences reach values of up to 40% (**Figure 5**). Differences may partially originate from larger uncertainties when fitting the auto-correlation functions to extract the viscosity due to larger fluctuations at high temperature (**Figure 1D**). In contrast, while the experimental data by Dobson et al. (1996) for KC melts are in strikingly good agreement with the MD results, those of KM melts are substantially lower than the theoretical predictions (**Figure 5**). Moreover, Dobson et al. (1996) reported negligible pressure effects on the viscosity of both compositions contrarily to the present results (**Figure 3**) and those of Desmaele et al. (2019b). The contrasting results for KM melt could be partially reconciled considering the large uncertainties (~50%) estimated for the experimental results (Dobson et al., 1996), although possible experimental shortcomings cannot be excluded. We note for instance inconsistencies in the experimental viscosity dataset for high K-carbonate melts from the same study - KM and $25MgCO_3$ - $75K_2CO_3$ melts - (**Figure 5**) that could result from incomplete melting of the samples and/or convection in the high pressure cell as recognized by the authors (Dobson et al., 1996), as well as from limitations in the detection of the falling-sphere (Kono et al., 2014; Stagno et al., 2018) and/or possible sample decomposition/contamination. In particular, hydration of the highly hygroscopic KM samples and/or boron contamination from the assembly (Malfait et al., 2014) that would both decrease the viscosity of the melt cannot be ruled out because detailed analysis of the recovered samples are not reported by Dobson et al. (1996).

Further, we employ the data to implement a model for the pressure-temperature dependence of the viscosity of KM and KC melts at upper mantle conditions. Among the different equations commonly employed to describe the non-Arrhenian temperature dependence of the viscosity (e.g.



Richet, 1984; Giordano and Dingwell, 2003; Russell et al., 2003), the Vogel-Fulcher-Tammann (VFT) equation (Vogel, 1921; Angell, 1995) was selected here owing to its ability to fit viscosity data over a wide range of temperature and to its empirical character:

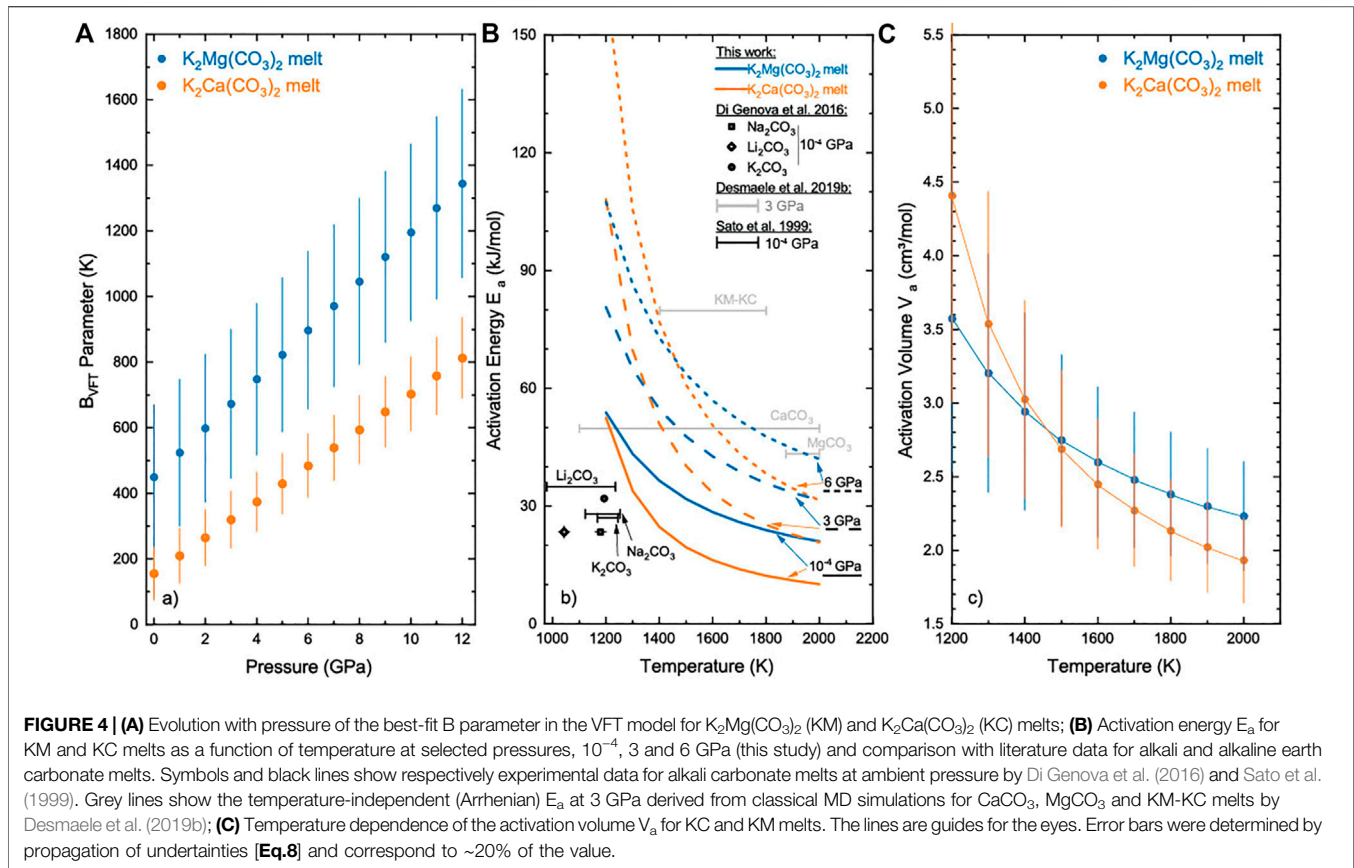
$$\log \eta = A_{VFT} + \left(\frac{B_{VFT}}{T - T_{VFT}} \right) \quad (5)$$

where A_{VFT} is the pre-exponential factor and represents the viscosity at infinite temperature, i.e. the high temperature limit to viscosity, B_{VFT} is a fitting parameter (in K) related to the pseudo-activation energy for viscous flow, i.e. RB_{VFT} (in J/mol, with R the ideal gas constant, 8.314 J/mol.K), which represents the resistance to the structural rearrangement of the melt (Richet, 1984; Bottinga and Richet, 1995), and T_{VFT} is the temperature at which the viscosity becomes infinite (i.e. temperature of divergence).

The $\log \eta$ -(P,T) datasets for each melt composition (i.e. 53 viscosity data points each, Table 2) were thus fitted to the VFT equation including an expansion of the B_{VFT} term to parametrize the effects of pressure on melt viscosity as:

$$\log \eta = A_{VFT} + \left(\frac{B_1 + B_2 P}{T - T_{VFT}} \right) \quad (6)$$

where B_1 and B_2 are adjustable parameters and P is the pressure, in bar. The VFT coefficients were optimized by using a non-linear regression routine to minimize the differences between predicted viscosities, i.e. by [Eq. 6], and the original viscosity datasets (Table 2). Uncertainties associated with the fitting parameters were obtained by the bootstrap resampling method, where the original datasets were randomly resampled 100,000 + 1 times and the optimized VFT parameters processed to derive the 95% confidence intervals (Supplementary Note S1). The best-fit VFT parameters [Eq. 6] derived on the original datasets for



each melt composition are reported in **Table 3** along with their uncertainties. The VFT models reproduce the original databases (**Table 2**) with average residuals of ± 0.05 and ± 0.04 log units for KM and KC melts, respectively, and associated average relative errors of 3 and 2.2% and Root Mean Square Errors (RMSE) of 0.06 and 0.05, that support the goodness of the fits. Moreover, the random distribution of the residuals over the databases further indicates the lack of systematic errors with either pressure or temperature in the calibration (**Supplementary Figure.S1**). Attempts to fit the temperature-dependence of the KM and KC viscosity datasets by an Arrhenian model result in lower reproducibility of the datasets (**Supplementary Figures S2–S4**) as shown by the goodness of fit metrics (**Supplementary Table S1**). Additional details of the quantitative comparison between the VFT and Arrhenian fit models, which confirms the non-Arrhenian behaviour of alkali(ne) carbonate melts over the investigated P-T conditions, are provided in Supplementary Note 1.

The optimal value of A_{VFT} parameter for KM and KC melts in the preferred VFT model, $-2.62^{+0.18}_{-0.15}$ and $-2.41^{+0.09}_{-0.09}$ respectively, agree well within mutual uncertainties, and suggest a compositional independent infinite temperature viscosity for carbonate melts as observed for silicate melts (e.g. Giordano and Dingwell, 2003; Russell et al., 2003; Giordano et al., 2008). Nevertheless, additional viscosity data over a broader P-T-compositional range would be required to validate this observation. The linear increase of the B_{VFT} parameter with

increasing pressure (**Figure 4A**), and hence of the pseudo-activation energy RB_{VFT} , suggests a progressive hindering of structural rearrangements in the melt at high pressure (Richet, 1984; Bottinga and Richet, 1995). At ambient pressure, the derived pseudo-activation energies for KM and KC melts, respectively $3,740^{+1840}_{-1746}$ and $1,290^{+765}_{-557}$ J/mol, are significantly lower than the range of values reported for silicate melts, 4,000–12,000 J/mol (Russell et al., 2003; Giordano et al., 2008; Li et al., 2021). The best-fit T_{VFT} values, 720^{+147}_{-104} and 914^{+90}_{-86} for KM and KC, respectively, fall below the corresponding liquidus temperatures at ambient pressure, 870–900 K for KM (Ragone et al., 1966) and ca. 1080 K for KC (Cooper et al., 1975).

The activation energy, E_a , which depends on both pressure and temperature, is further calculated from the slope of the curves in **Figure 3**, obtained by differentiating $\log \eta$ as provided by **Eq. 6** with respect to $1/T$ following:

$$E_a = 2.303R \frac{\partial \log \eta}{\partial (1/T)} = 2.303R(B_1 + B_2 \cdot P) \left(\frac{T}{(T - T_{VFT})} \right)^2 \quad (7)$$

where R is the gas constant, 8.314 J/mol.K, and the B_1 , B_2 and T_{VFT} parameters for each melt composition are taken from **Table 3**. The activation energy E_a values for both KM and KC melts are reported in **Figure 4** as a function of temperature at selected pressures, i.e. ambient, 3 and 6 GPa. The activation energy E_a decreases with temperature regardless of pressure and/or melt composition, in agreement with the decrease of

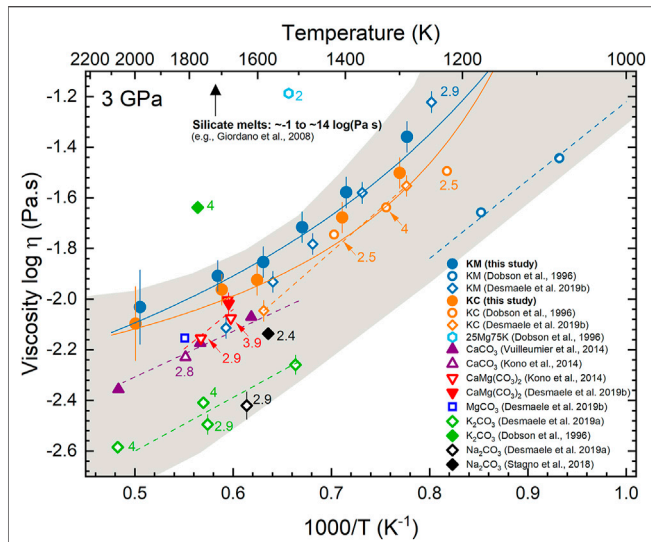


FIGURE 5 | Effect of temperature on the viscosity of $K_2Mg(CO_3)_2$ (KM, blue) and $K_2Ca(CO_3)_2$ (KC, orange) melts from this MD study (full circles) and comparison with literature data for alkali and alkaline carbonate melts. All data are reported at 3 GPa unless indicated next to the symbols (in GPa). Solid lines represent fits to the temperature dependence of the viscosity data by the VFT model (present data) and dashed lines by an Arrhenian model (literature data). Errors bars on KM, KC and K_2CO_3 melts from Dobson et al. (1996) correspond to 50% (not shown for the sake of clarity). Viscosities of silicate melts are indicated for comparison (Giordano et al., 2008).

the energy barrier for viscous flow at higher temperature (Bottinga and Richet, 1995). The effect of temperature on E_a is, however, more pronounced at higher pressures (Figure 4B). The ambient pressure activation energies derived here for KM and KC melts are higher than typical values for alkali carbonates melts, i.e. K_2CO_3 , Na_2CO_3 and Li_2CO_3 (24–35 kJ/mol), as determined by experimental studies at 1,050–1,200 K (Sato et al., 1999; Di Genova et al., 2016) and classical MD simulations (Desmaele et al., 2019a) in the 1,100–1,900 K temperature range (Figure 4B). Our results at 3 GPa and low temperature compare well with the constant (i.e. Arrhenian) E_a of 80 kJ/mol reported for KM and KC melts at the same pressure in Desmaele et al. (2019b), although differences increase with temperature as the VFT model predicts a decrease of E_a down to ~20–30 kJ/mol at 2,000 K. Moreover, the activation energies for KM and KC melts are generally larger than those calculated for the end-members $CaCO_3$ and $MgCO_3$ melts (43–49 kJ/mol) at similar P-T conditions (Desmaele et al., 2019b), consistent with the compositional effects discussed in detail below (Figure 5).

Pressure appears to have a non-negligible effect on the calculated viscosity of alkali(ne) carbonate melts (Figure 4) in contrast with the reports from experimental studies (Dobson et al., 1996; Kono et al., 2014; Stagno et al., 2018). We suggest that the large uncertainties in early viscosity measurements, 50% (Dobson et al., 1996), and the limited viscosity datasets reported in recent studies (Kono et al., 2014; Stagno et al., 2018), do not allow resolving pressure effects. Contrary to temperature, the pressure dependence of the viscosity is linear within the uncertainties (Figure 3). The activation volume of viscous flow, V_a , can be derived from the pressure effect on viscosity by differentiating Eq. 6 as:

TABLE 3 | Best-fit parameters for the Vogel-Fulcher-Tammann (VFT) model [Eq. 6] fitted to the pressure-temperature dependence of the viscosity of $K_2Mg(CO_3)_2$ (KM) and $K_2Ca(CO_3)_2$ (KC) melts.

VFT parameter	KM melt	KC melt
A_{VFT} (Pa s)	$-2.62^{+0.18}_{-0.15}$	$-2.41^{+0.09}_{-0.09}$
B_1 (K)	449^{+221}_{-210}	155^{+82}_{-67}
B_2 (K/bar)	$0.0075^{+0.0008}_{-0.0013}$	$0.0055^{+0.0006}_{-0.0008}$
T_{VFT} (K)	720^{+147}_{-104}	914^{+90}_{-86}
Residual ^a	±0.05	±0.04
Rel. error ^b (%)	3.0	2.2
RMSE ^c	0.06	0.05

¹Average residual = $\langle |observed - predicted| \rangle$ (in log units).

²Average relative error = $\langle |observed - predicted| / observed \rangle \times 100$ (in %).

³Average Root Mean Square Error = $\sqrt{\frac{1}{n} \sum_{i=1}^n (Observed - Predicted)^2}$ (in log units).

$$V_a = 2.303RT \frac{\partial \log \eta}{\partial P} = 2.303RT \frac{B_2}{(T - T_{VFT})} \quad (8)$$

where R is the gas constant, and the parameters T_{VFT} and B_2 are provided in Table 3 for each melt composition. The activation volumes V_a derived for both KM and KC melts are positive at all investigated temperatures, and range from 4.5–3.5 cm^3/mol at 1,300 K to ~2–1.9 cm^3/mol at 2,000 K (Figure 4C). These V_a values are consistent with those reported in previous MD simulations for alkali and alkaline-earth carbonate melts, i.e. 2.2–4.7 cm^3/mol (Desmaele et al., 2019a; 2019b). The results also compare well with the V_a values for $CaCO_3$ - $CaMg(CO_3)_2$ melts retrieved using the experimental viscosity model of Kono et al. (2014) and Eq. 8, i.e. 3.6 cm^3/mol and 1.1 cm^3/mol at 1,600 and 1,800 K, respectively. Conversely, Stagno et al. (2018) reported an activation volume from viscosity measurements on Na_2CO_3 melt, $V_a = 54.52 cm^3/mol$, which is an order of magnitude larger than the results discussed above. We note however that this value does not represent the activation volume due to the non-Arrhenian fit model employed in the data analysis and therefore cannot be directly compared to the results obtained here. Additional inconsistencies in the Na_2CO_3 melt viscosity model, including for instance a temperature of divergence of the viscosity (i.e. T_0 in Stagno et al. (2018)) that is larger than the lowest temperature investigated and hence implies the divergence of the predicted viscosity on the calibration temperature interval, preclude the use of the fitting parameters to retrieve the V_a [Eq. 8] for comparison. These issues will be addressed in a Corrigendum that is currently in preparation (V. Stagno, pers. comm). The trend that emerges from the available data on the activation volume V_a of viscous flow of carbonate melts is that they are positive at mantle conditions and comparable with typical values reported for intermediate polymerized to depolymerized silicate melts, $V_a \sim 2$ –6 cm^3/mol at 1,800–2,000 K (e.g. Liesbke et al., 2005; Rai et al., 2019; Li et al., 2021).

Compositional Effects on the Viscosity of Alkali(ne) Carbonate Melts

The viscosities of KM and KC melts at 3 GPa and various temperatures are compared to available data at similar conditions for alkali and alkaline earth (and mixtures thereof) carbonate melts

from experiments and MD simulations in **Figure 5**. Most carbonate melt viscosities reported to date fall between -2.6 and -1.2 on the logarithmic scale, which is generally several orders of magnitude lower compared to silicate melts (e.g. Giordano and Dingwell, 2003; Liebske et al., 2005; Giordano et al., 2008; Wang et al., 2014). The viscosities of K_2CO_3 melt at 4 GPa and $25\text{MgCO}_3\text{-}75\text{K}_2\text{CO}_3$ melt at 2 GPa reported by Dobson et al. (1996) are significantly larger than those of the whole data sets and likely overestimated as discussed above.

Although specific compositional effects on the viscosity of carbonate melts are difficult to assess at this stage due to the limited datasets available and the inconsistencies between studies (**Figure 5**), some general trends can be identified. Molten CaCO_3 , MgCO_3 and $\text{CaMg}(\text{CO}_3)_2$ show similar viscosities (Kono et al., 2014; Vuilleumier et al., 2014; Desmaele et al., 2019a, 2019b), which are larger than the viscosity of alkali carbonate melts, such as K_2CO_3 or Na_2CO_3 , reported from MD studies by Desmaele et al. (2019a). Interestingly, the viscosity of KM and KC melts from this study and that of Desmaele et al., 2019b is larger than the viscosities of the corresponding alkali and alkaline earth end-members (**Figure 5**). Although this result may appear counter-intuitive, experimental studies show that the viscosity of binary ionic liquid mixtures can be higher or lower than the viscosity of the end-members, or close to their arithmetic mean (Fillon and Brennecke, 2017). The enhanced viscosity of KC and KM melts compared to the end-members likely results from the increase in Coulombic interactions between the metal cations (i.e. Ca, Mg, K) and/or carbonate groups upon mixing that will modify the charge distributions and enhance the dynamics in the system, hence increasing the viscosity (Wilson et al., 2018). Additionally, we note that the experimental viscosities of Na_2CO_3 melt (Stagno et al., 2018) are substantially larger than the results from MD simulations (Desmaele et al., 2019a) but comparable to those of calcitic, magnesian and dolomitic melts at similar pressures (Kono et al., 2014; Vuilleumier et al., 2014; Desmaele et al., 2019b). The origin of the discrepancies between simulated and experimental viscosities of Na_2CO_3 melt is, however, difficult to identify within the available data. With the exception of the results from Stagno et al., (2018), the data reported in **Figure 5** suggest that alkali elements (i.e. Na and K) play a crucial role in modifying the viscosity of carbonate melt. This effect may result from the larger ionic radii of alkalis (Di Genova et al., 2016; Stagno et al., 2018) and/or enhanced interactions with alkaline elements upon substitution as discussed above. In contrast, the limited compositional effects on the viscosity of alkaline earth carbonate melts, $\text{CaCO}_3\text{-CaMg}(\text{CO}_3)_2$ (and likely MgCO_3) melts (**Figure 5**), upon Ca and Mg exchange reflect their structural similarities, with only minor differences in the interatomic distances as shown by X-ray diffraction studies (Kono et al., 2014). The effect of potassium on the viscosity of alkaline carbonate melts contrasts with its role in silicate melts, where the viscosity increases upon increasing the field strength of the network-stabilizing cation following the trend: $\eta_{\text{K}^+} < \eta_{\text{Na}^+} < \eta_{\text{Sr}^+} < \eta_{\text{Ca}^{2+}} < \eta_{\text{Mg}^{2+}}$ (Dingwell, 2007). Contrary to previous reports (Kono et al., 2014; Stagno et al., 2018), the data reported in **Figure 5** reveal compositional effects on the viscosity of alkali(ne) carbonate melts, despite the limitations to identify clear trends. Additional data on the viscosity of alkali(ne) carbonate melts, including a broad range of mixed compositions in the systems $\text{MgCO}_3\text{-CaCO}_3\text{-K}_2\text{CO}_3\text{-Na}_2\text{CO}_3$ would be required to draw further conclusions.

Non-Arrhenian Viscosity of Carbonate Melts in the Mantle

The non-Arrhenian temperature-dependent viscosity (fragile behavior) reported here for alkali(ne) carbonate melts is somehow not unexpected as the departure from an exponential activation law (i.e. Arrhenian behavior) is a common feature for most melt/liquid systems investigated to date, including for a broad range of silicate melt compositions over geologically relevant temperature intervals (Richet, 1984; Angell, 1995; Webb, 1997). Notable exceptions to this trend are highly polymerized silicate melts (i.e. strong melts, Angell, 1995) such as SiO_2 and granitic-albitic melts that display Arrhenian behavior at all investigated temperature conditions (e.g. Richet, 1984; Webb, 1997; Giordano and Dingwell, 2003). The strong/fragile pattern reflects the sensitivity of the liquid/melt structure to temperature changes, which is in turn controlled by the structural arrangements and nature of bonding in the system (Angell, 1995). For silicate melts, there is a clear correlation between the melt fragility and the degree of polymerization defined by the NBO/T parameter (Giordano et al., 2013; Malfait and Sanchez-Valle, 2013). The fragility exhibited by carbonate melts may thus arise from their ionic nature, characterized by simple Coulomb interactions, that readily permit for a variety of particle orientations and coordination states to reorganize the structure in response to thermal perturbations. Recent MD simulations performed in molten Na_2CO_3 provide indeed evidence for the formation of low-dimensional structures in the CO_3^{2-} network (e.g. chains, triangles and tetrahedra) that are temperature dependent and change the melt dynamics and hence, enhance melt fragility (Wilding et al., 2016; Wilson et al., 2018). Note that pressure also favors the formation of extended low-dimensional networks of CO_3^{2-} pairs and the rise of CO_{3+1} local coordination environments in KM melt that result in an increase of melt viscosity with pressure (Wilding et al., 2019) consistent with the present observations (**Figure 3**).

The alkali(ne) carbonate melts investigated here are to date the only carbonate melt compositions displaying a non-Arrhenian temperature dependent viscosity (**Figure 5**), likely due to the limited temperature range investigated by previous studies (**Table 1**). Therefore, departures of the viscosity from the Arrhenian behavior may not be ruled out for other carbonate melt compositions as observed for silicate melts (e.g. Richet, 1984; Webb, 1997; Giordano and Dingwell, 2003). The present results thus advise against the application of a simple Arrhenian model to extrapolate over a broad range of temperature the available data for the viscosity of other carbonate melt compositions (**Figure 5**). This will predict changes in viscosity with temperature that are larger than indicated by the non-Arrhenian behavior observed here and, in turn, would result in underestimations of carbonate melt mobility in the upper mantle. This point is particularly critical when modeling carbonate magmatic processes at crustal and shallow upper mantle conditions (< 7 GPa), e.g. carbonate magma chamber dynamics or carbonate melt mobility beneath mid-oceanic ridges, as they span the conditions where the strongest non-Arrhenian behavior of the viscosity has been observed (**Figure 3**).

CONCLUSION

The viscosity of alkali(ne) carbonate melts, KM and KC, has been determined over a broad range of pressure and temperature conditions, i.e. from ambient pressure to 13 GPa and 1,000–2,000 K, by means of classical MD simulations. Both melt compositions are more viscous than alkaline carbonate melts, i.e. CaCO_3 , MgCO_3 and $\text{CaMg}(\text{CO}_3)_2$, likely due to the change in charge distribution upon potassium substitution. Temperature appears as the primary control parameter on the viscosity of alkali(ne) carbonate melts, even though pressure effects are not negligible in contrast with previous reports. Most interestingly, this study identifies for the first time non-Arrhenian temperature-dependent viscosities in carbonate melts at high pressure, while the viscosity increases linearly with pressure at all investigated conditions. The non-Arrhenian viscosity of KM and KC melts may arise from the formation of temperature-dependent low-dimensional structures in the melt that are more drastic in the carbonate network than in the cation network (Wilson et al., 2018). Therefore, the non-Arrhenian behaviour may be expected for other carbonate melt compositions regardless of the cation nature, although the experimental and/or theoretical confirmation is still awaiting. The present results might be taken into account when modeling the mobility of carbonate melts in the upper mantle.

DATA AVAILABILITY STATEMENT

The original contributions presented in the study are included in the article/**Supplementary Material**. The repository containing the output files from the MD simulations are available at: <https://uni-muenster.sciebo.de/s/N82lU5t1ejYFCq4>. Further inquiries can be directed to the corresponding author.

REFERENCES

- Angell, C. A. (1995). Formation of Glasses from Liquids and Biopolymers. *Science* 267, 1924–1935. doi:10.1126/science.267.5206.1924
- Boon, J.-P., and Yip, S. (1980). *Molecular Hydrodynamics*. Toronto: McGraw-Hill.
- Bottinga, Y., and Richet, P. (1995). Silicate Melts: The “Anomalous” Pressure Dependence of the Viscosity. *Geochimica et Cosmochimica Acta* 59, 2725–2731. doi:10.1016/0016-7037(95)00168-Y
- Cooper, A. F., Gittins, J., and Tuttle, O. F. (1975). The System Na_2CO_3 - K_2CO_3 - CaCO_3 at 1 Kilobar and its Significance in Carbonatite Petrogenesis. *Am. J. Sci.* 275, 534–560. doi:10.2475/ajs.275.5.534
- Corradini, D., Couderc, F.-X., and Vuilleumier, R. (2016). Insight into the Li_2CO_3 - K_2CO_3 Eutectic Mixture from Classical Molecular Dynamics: Thermodynamics, Structure, and Dynamics. *J. Chem. Phys.* 144, 104507. doi:10.1063/1.4943392
- Dalton, J. A., and Presnall, D. C. (1998). The Continuum of Primary Carbonatitic-Kimberlitic Melt Compositions in Equilibrium with Lherzolitite: Data from the System CaO - MgO - Al_2O_3 - SiO_2 - CO_2 at 6 GPa. *J. Petrol.* 39, 1953–1964. doi:10.1093/ptroj/39.11-12.1953
- Dasgupta, R., and Hirschmann, M. M. (2010). The Deep Carbon Cycle and Melting in Earth's interior. *Earth Planet. Sci. Lett.* 298, 1–13. doi:10.1016/j.epsl.2010.06.039
- Dasgupta, R. (2013). Ingressing, Storage, and Outgassing of Terrestrial Carbon through Geologic Time. *Rev. Mineralogy Geochem.* 75, 183–229. doi:10.2138/rmg.2013.75.7
- Desmaele, E., Sator, N., Vuilleumier, R., and Guillot, B. (2019a). Atomistic Simulations of Molten Carbonates: Thermodynamic and Transport Properties of the Li_2CO_3 - Na_2CO_3 - K_2CO_3 System. *J. Chem. Phys.* 150, 094504. doi:10.1063/1.5082731
- Desmaele, E., Sator, N., Vuilleumier, R., and Guillot, B. (2019b). The MgCO_3 - CaCO_3 - Li_2CO_3 - Na_2CO_3 - K_2CO_3 Melts: Thermodynamics and Transport Properties by Atomistic Simulations. *J. Chem. Phys.* 150, 214503. doi:10.1063/1.5099015
- Di Genova, D., Cimarelli, C., Hess, K.-U., and Dingwell, D. B. (2016). An Advanced Rotational Rheometer System for Extremely Fluid Liquids up to 1273 K and Applications to Alkali Carbonate Melts. *Am. Mineral.* 101, 953–959. doi:10.2138/am-2016-5537CCBYNCND
- Dingwell, D. B. (2007). Properties of Rocks and Minerals - Diffusion, Viscosity, and Flow of Melts. *Treatise Geophys.* 2, 419–436. doi:10.1016/B978-0-44452748-6.00044-4
- Dingwell, D. B., and Webb, S. L. (1989). Structural Relaxation in Silicate Melts and Non-Newtonian Melt Rheology in Geologic Processes. *Phys. Chem. Minerals* 16, 508–516. doi:10.1007/bf00197020
- Dixon, J. E., Clague, D. A., Cousens, B., Monsalve, M. L., and Uhl, J. (2008). Carbonatite and Silicate Melt Metasomatism of the Mantle Surrounding the Hawaiian Plume: Evidence from Volatiles, Trace Elements, and Radiogenic Isotopes in Rejuvenated-Stage Lavas from Niihau, Hawaii. *Geochem. Geophys. Geosystems* 9, 1–34. doi:10.1029/2008gc002076
- Dobson, D. P., Jones, A. P., Rabe, R., Sekine, T., Kurita, K., Taniguchi, T., et al. (1996). *In-Situ* Measurement of Viscosity and Density of Carbonate Melts at

AUTHOR CONTRIBUTIONS

CS-V, BG and NS organized the project, XR performed the MD simulations in collaboration with BG and NS, ED implemented the force fields, CS-V, XR and MM processed the data and CS-V and XR wrote the manuscript with input from all the authors.

FUNDING

This research was funded through the German Science Foundation (DFG grant SA 2585/4-1 to CS-V), start-up funds from WWU Münster, a mobility grant from the DAAD (ref. no. 57381316 to XR) and the H2020-MSCA project MoVEMENT (grant No. 842339 to MM).

ACKNOWLEDGMENTS

XR acknowledges financial support from the DAAD for a 6 months stay at Sorbonne University Paris to perform the MD simulations (ref. no. 57381316). MM acknowledges support from the European Union's Horizon 2020 research and innovation program under the Marie Skłodowska-Curie Actions (grant agreement No. 842339). We thank the two reviewers for their comments and the Associate Editor M. Mookherjee for editorial handling.

SUPPLEMENTARY MATERIAL

The Supplementary Material for this article can be found online at: <https://www.frontiersin.org/articles/10.3389/feart.2021.674770/full#supplementary-material>.

- High Pressure. *Earth Planet. Sci. Lett.* 143, 207–215. doi:10.1016/0012-821X(96)00139-2
- Dufils, T., Folliet, N., Mantsi, B., Sator, N., and Guillot, B. (2017). Properties of Magmatic Liquids by Molecular Dynamics Simulation: The Example of a MORB Melt. *Chem. Geology*. 461, 34–46. doi:10.1016/j.chemgeo.2016.06.030
- Dufils, T., Sator, N., and Guillot, B. (2018). Properties of Planetary Silicate Melts by Molecular Dynamics Simulation. *Chem. Geology*. 493, 298–315. doi:10.1016/j.chemgeo.2018.06.003
- Fillon, J. J., and Brennecke, J. F. (2017). Viscosity of Ionic Liquid-Ionic Liquid Mixtures. *J. Chem. Eng. Data* 62, 1884–1901. doi:10.1021/acs.jced.7b00221
- Fischer, K. M., Ford, H. A., Abt, D. L., and Rychert, C. A. (2010). The Lithosphere-Asthenosphere Boundary. *Annu. Rev. Earth Planet. Sci.* 38, 551–575. doi:10.1146/annurev-earth-040809-152438
- Gaillard, F., Malki, M., Iacono-Marziano, G., Pichavant, M., and Scaillet, B. (2008). Carbonatite Melts and Electrical Conductivity in the Asthenosphere. *Science* 322, 1363–1365. doi:10.1126/science.1164446
- Gardés, E., Laumonier, M., Massuyeau, M., and Gaillard, F. (2020). Unravelling Partial Melt Distribution in the Oceanic Low Velocity Zone. *Earth Planet. Sci. Lett.* 540, 116242. doi:10.1016/j.epsl.2020.116242
- Genge, M. J., Price, G. D., and Jones, A. P. (1995). Molecular Dynamics Simulations of CaCO₃ Melts to Mantle Pressures and Temperatures: Implications for Carbonatite Magmas. *Earth Planet. Sci. Lett.* 131, 225–238. doi:10.1016/0012-821X(95)00020-D
- Gervasoni, F., Klemme, S., Rohrbach, A., Grützner, T., and Berndt, J. (2017). Experimental Constraints on Mantle Metasomatism Caused by Silicate and Carbonate Melts. *Lithos* 282–283, 173–186. doi:10.1016/j.lithos.2017.03.004
- Giordano, D., and Dingwell, D. B. (2003). Non-Arrhenian Multicomponent Melt Viscosity: A Model. *Earth Planet. Sci. Lett.* 208, 337–349. doi:10.1016/S0012-821X(03)00042-6
- Giordano, D., Russell, J. K., and Dingwell, D. B. (2008). Viscosity of Magmatic Liquids: A Model. *Earth Planet. Sci. Lett.* 271, 123–134. doi:10.1016/j.epsl.2008.03.038
- Glasstone, S., Laidler, K. J., and Eyring, H. (1941). *The Theory of Rate Processes*. New York: McGraw-Hill.
- Grassi, D., and Schmidt, M. W. (2011a). Melting of Carbonated Pelites at 8–13 GPa: Generating K-Rich Carbonatites for Mantle Metasomatism. *Contrib. Mineral. Petrol.* 162, 169–191. doi:10.1007/s00410-010-0589-9
- Grassi, D., and Schmidt, M. W. (2011b). The Melting of Carbonated Pelites from 70 to 700 Km Depth. *J. Petrol.* 52, 765–789. doi:10.1093/petrology/egr002
- Green, D. H., and Wallace, M. E. (1988). Mantle Metasomatism by Ephemeral Carbonatite Melts. *Nature* 336, 459–462. doi:10.1038/336459a0
- Gudfinnsson, G. H., and Presnall, D. C. (2005). Continuous Gradations Among Primary Carbonatitic, Kimberlitic, Melilititic, Basaltic, Picritic, and Komatiitic Melts in Equilibrium with Garnet Lherzolite at 3–8 GPa. *J. Petrol.* 46, 1645–1659. doi:10.1093/petrology/egi029
- Guillot, B., and Sator, N. (2007a). A Computer Simulation Study of Natural Silicate Melts. Part I: Low Pressure Properties. *Geochimica et Cosmochimica Acta* 71, 1249–1265. doi:10.1016/j.gca.2006.11.015
- Guillot, B., and Sator, N. (2007b). A Computer Simulation Study of Natural Silicate Melts. Part II: High Pressure Properties. *Geochimica et Cosmochimica Acta* 71, 4538–4556. doi:10.1016/j.gca.2007.05.029
- Guillot, B., and Sator, N. (2011). Carbon Dioxide in Silicate Melts: A Molecular Dynamics Simulation Study. *Geochimica et Cosmochimica Acta* 75, 1829–1857. doi:10.1016/j.gca.2011.01.004
- Hammouda, T., and Keshav, S. (2015). Melting in the Mantle in the Presence of Carbon: Review of Experiments and Discussion on the Origin of Carbonatites. *Chem. Geology*. 418, 171–188. doi:10.1016/j.chemgeo.2015.05.018
- Hammouda, T., and Laporte, D. (2000). Ultrafast Mantle Impregnation by Carbonatite Melts. *Geology* 28, 283–285. doi:10.1130/0091-7613(2000)028<0283:umibcm>2.3.co;2
- Hess, B. (2002). Determining the Shear Viscosity of Model Liquids from Molecular Dynamics Simulations. *J. Chem. Phys.* 116, 209. doi:10.1063/1.1421362
- Hurt, S. M., and Wolf, A. S. (2019). Thermodynamic Properties of CaCO₃-SrCO₃-BaCO₃ Liquids: a Molecular Dynamics Study Using New Empirical Atomic Potentials for Alkaline Earth Carbonates. *Phys. Chem. Minerals* 46, 165–180. doi:10.1007/s00269-018-0995-5
- Janz, G. J. (1988). Thermodynamic and Transport Properties for Molten Salts: Correlation Equations for Critically Evaluated Density, Surface Tension, Electrical Conductance, and Viscosity Data. *J. Phys. Chem. Ref. Data* 17, 325.
- Jones, A. P., Genge, M., and Carmody, L. (2013). Carbonate Melts and Carbonatites. *Rev. Mineralogy Geochem.* 75, 289–322. doi:10.2138/rmg.2013.75.10
- Keller, T., Katz, R. F., and Hirschmann, M. M. (2017). Volatiles Beneath Mid-Ocean Ridges: Deep Melting, Channelised Transport, Focusing, and Metasomatism. *Earth Planet. Sci. Lett.* 464, 55–68. doi:10.1016/j.epsl.2017.02.006
- Kiseeva, E. S., Litasov, K. D., Yaxley, G. M., Ohtani, E., and Kamenetsky, V. S. (2013). Melting and Phase Relations of Carbonated Eclogite at 9–21 GPa and the Petrogenesis of Alkali-Rich Melts in the Deep Mantle. *J. Petrol.* 54, 1555–1583. doi:10.1093/petrology/egt023
- Kiseeva, E. S., Yaxley, G. M., Hermann, J., Litasov, K. D., Rosenthal, A., and Kamenetsky, V. S. (2012). An Experimental Study of Carbonated Eclogite at 3 {middle Dot}5–5{middle Dot}5 GPa—Implications for Silicate and Carbonate Metasomatism in the Cratonic Mantle. *J. Petrol.* 53, 727–759. doi:10.1093/petrology/egr078
- Kojima, T. (2009). *Physical and Chemical Properties of Molten Carbonates*. PhD Thesis, Kobe University.
- Kono, Y., Kenney-Benson, C., Hummer, D., Ohfuji, H., Park, C., Shen, G., et al. (2014). Ultralow Viscosity of Carbonate Melts at High Pressures. *Nat. Commun.* 5, 5091. doi:10.1038/ncomms6091
- Korsakov, A. V., and Hermann, J. (2006). Silicate and Carbonate Melt Inclusions Associated with Diamonds in Deeply Subducted Carbonate Rocks. *Earth Planet. Sci. Lett.* 241, 104–118. doi:10.1016/j.epsl.2005.10.037
- Kubicki, J. D., and Lasaga, A. C. (1988). Molecular Dynamics Simulations of SiO₂ Melt and Glass: Ionic and Covalent Models. *Am. Mineral.* 73, 941–955.
- Li, M., Russell, J. K., and Giordano, D. (2021). Temperature-Pressure-Composition Model for Melt Viscosity in the Di-an-ab System. *Chem. Geology*. 560, 119895. doi:10.1016/j.chemgeo.2020.119895
- Li, Z., Li, J., Lange, R., Liu, J., and Militzer, B. (2017). Determination of Calcium Carbonate and Sodium Carbonate Melting Curves up to Earth's Transition Zone Pressures with Implications for the Deep Carbon Cycle. *Earth Planet. Sci. Lett.* 457, 395–402. doi:10.1016/j.epsl.2016.10.027
- Liebske, C., Schmickler, B., Terasaki, H., Poe, B., Suzuki, A., Funakoshi, K., et al. (2005). Viscosity of Peridotite Liquid up to 13 GPa: Implications for Magma Ocean Viscosities. *Earth Planet. Sci. Lett.* 240, 589–604. doi:10.1016/j.epsl.2005.10.004
- Liu, Q., and Lange, R. A. (2003). New Density Measurements on Carbonate Liquids and the Partial Molar Volume of the CaCO₃ Component. *Contrib. Mineralogy Petrology*. 146, 370–381. doi:10.1007/s00410-003-0505-7
- Malfait, W. J., and Sanchez-Valle, C. (2013). Effect of Water and Network Connectivity on Glass Elasticity and Melt Fragility. *Chem. Geology*. 346, 72–80. doi:10.1016/j.chemgeo.2012.04.034
- Malfait, W. J., Seifert, R., Petitgirard, S., Mezour, M., and Sanchez-Valle, C. (2014). The Density of Andesitic Melts and the Compressibility of Dissolved Water in Silicate Melts at Crustal and Upper Mantle Conditions. *Earth Planet. Sci. Lett.* 393, 31–38. doi:10.1016/j.epsl.2014.02.042
- Massuyeau, M., Gardés, E., Rogerie, G., Aulbach, S., Tappe, S., Le Trong, E., et al. (2021). MAGLAB: A Computing Platform Connecting Geophysical Signatures to Melting Processes in Earth's Mantle. *Phys. Earth Planet. Interiors* 314, 106638. doi:10.1016/j.pepi.2020.106638
- Minarik, W. G., and Watson, E. B. (1995). Interconnectivity of Carbonate Melt at Low Melt Fraction. *Earth Planet. Sci. Lett.* 133, 423–437. doi:10.1016/0012-821X(95)00085-Q
- Naif, S., Key, K., Constable, S., and Evans, R. L. (2013). Melt-Rich Channel Observed at the Lithosphere-Asthenosphere Boundary. *Nature* 495, 356–359. doi:10.1038/nature11939
- O'Leary, M. C., Lange, R. A., and Ai, Y. (2015). The Compressibility of CaCO₃-Li₂CO₃-Na₂CO₃-K₂CO₃ Liquids: Application to Natrocarbonatite and CO₂-Bearing Nephelinite Liquids from Oldoinyo Lengai. *Contrib. Mineral. Petrol.* 170, 3. doi:10.1007/s00410-015-1157-0
- Poli, S. (2015). Carbon Mobilized at Shallow Depths in Subduction Zones by Carbonatitic Liquids. *Nat. Geosci.* 8, 633–636. doi:10.1038/ngeo2464
- Ragone, S. E., Datta, R. K., Roy, D. M., and Tuttle, O. F. (1966). The System Potassium Carbonate-Magnesium Carbonate. *J. Phys. Chem.* 70, 3360–3361. doi:10.1021/j100882a515

- Rai, N., Perrillat, J.-P., Mezouar, M., Colin, A., Petitgirard, S., and van Westrenen, W. (2019). *In Situ* Viscometry of Primitive Lunar Magmas at High Pressure and High Temperature. *Front. Earth Sci.* 7 (1-12), 94. doi:10.3389/feart.2019.00094
- Richet, P. (1984). Viscosity and Configurational Entropy of Silicate Melts. *Geochimica et Cosmochimica Acta* 48, 471–483. doi:10.1016/0016-7037(84)90275-8
- Ritter, X., Sanchez-Valle, C., Sator, N., Desmaele, E., Guignot, N., King, A., et al. (2020). Density of Hydrous Carbonate Melts under Pressure, Compressibility of Volatiles and Implications for Carbonate Melt Mobility in the Upper Mantle. *Earth Planet. Sci. Lett.* 533, 116043. doi:10.1016/j.epsl.2019.116043
- Rudnick, R. L., McDonough, W. F., and Chappell, B. W. (1993). Carbonatite Metasomatism in the Northern Tanzanian Mantle: Petrographic and Geochemical Characteristics. *Earth Planet. Sci. Lett.* 114, 463–475. doi:10.1016/0012-821X(93)90076-L
- Russell, J. K., Giordano, D., and Dingwell, D. B. (2003). High-Temperature Limits on Viscosity of Non-Arrhenian Silicate Melts. *Am. Mineral.* 88, 1390–1394. doi:10.2138/am-2003-8-924
- Russell, J. K., Porritt, L. A., Lavallée, Y., and Dingwell, D. B. (2012). Kimberlite Ascent by Assimilation-Fuelled Buoyancy. *Nature* 481, 352–356. doi:10.1038/nature10740
- Rustad, J. R., Yuen, D. A., and Spera, F. J. (1990). Molecular Dynamics of liquid SiO₂ under High Pressure. *Phys. Rev. A* 42, 2081–2089. doi:10.1103/physrevA.42.2081
- Sato, Y., Yaegashi, S., Kijima, T., Takeuchi, E., Tamai, K., Hasebe, M., et al. (1999). Viscosities of Molten Alkali Carbonates. *Jpn. J. Thermophys. Prop.* 13, 156–161. doi:10.2963/jjtp.13.156
- Shatskiy, A. F., Litasov, K. D., and Palyanov, Y. N. (2015). Phase Relations in Carbonate Systems at Pressures and Temperatures of Lithospheric Mantle: Review of Experimental Data. *Russ. Geol. Geophys.* 56, 113–142. doi:10.1016/j.rgg.2015.01.007
- Sifré, D., Gardés, E., Massuyeau, M., Hashim, L., Hier-Majumder, S., and Gaillard, F. (2014). Electrical Conductivity during Incipient Melting in the Oceanic Low-Velocity Zone. *Nature* 509, 81–85. doi:10.1038/nature13245
- Smith, W., and Forester, T. R. (1996). DL_POLY_2.0: A General-Purpose Parallel Molecular Dynamics Simulation Package. *J. Mol. Graphics* 14, 136–141. doi:10.1016/S0263-7855(96)00043-4
- Sparks, R. S. J. (2013). Kimberlite Volcanism. *Annu. Rev. Earth Planet. Sci.* 41, 497–528. doi:10.1146/annurev-earth-042711-105252
- Stagno, V. (2019). Carbon, Carbides, Carbonates and Carbonatitic Melts in the Earth's interior. *J. Geol. Soc.* 176, 375–387. doi:10.1144/jgs2018-095
- Stagno, V., Stopponi, V., Kono, Y., Manning, C. E., and Irifune, T. (2018). Experimental Determination of the Viscosity of Na₂CO₃ Melt between 1.7 and 4.6 GPa at 1,200–1700 °C: Implications for the Rheology of Carbonatite Magmas in the Earth's Upper Mantle. *Chem. Geology* 501, 19–25. doi:10.1016/j.chemgeo.2018.09.036
- Sun, C., and Dasgupta, R. (2019). Slab-Mantle Interaction, Carbon Transport, and Kimberlite Generation in the Deep Upper Mantle. *Earth Planet. Sci. Lett.* 506, 38–52. doi:10.1016/j.epsl.2018.10.028
- Tissen, J. T. W. M., Janssen, G. J. M., and Eerden, P. V. D. (1994). Molecular Dynamics Simulation of Binary Mixtures of Molten Alkali Carbonates. *Mol. Phys.* 82, 101–111. doi:10.1080/00268979400100084
- Treiman, A. H. (1995). Ca-rich Carbonate Melts; a Regular-Solution Model, with Application to Carbonatite Magma + Vapor Equilibria and Carbonate Lavas on Venus. *Am. Mineral.* 80, 115–130. doi:10.2138/am-1995-1-212
- Treiman, A. H., and Schedl, A. (1983). Properties of Carbonatite Magma and Processes in Carbonatite Magma Chambers. *J. Geology* 91, 437–447. doi:10.1086/628789
- Veksler, I. V., Petibon, C., Jenner, G. A., Dorfman, A. M., and Dingwell, D. B. (1998). Trace Element Partitioning in Immiscible Silicate-Carbonate Liquid Systems: an Initial Experimental Study Using a Centrifuge Autoclave. *J. Petrol.* 39, 2095–2104. doi:10.1093/ptro/39.11-12.2095
- Vogel, D. H. (1921). Das Temperaturabhängigkeitsgesetz der Viskosität von Flüssigkeiten. *Phys. Z.* 22, 645.
- Vuilleumier, R., Seitsonen, A., Sator, N., and Guillot, B. (2014). Structure, Equation of State and Transport Properties of Molten Calcium Carbonate (CaCO₃) by Atomistic Simulations. *Geochimica et Cosmochimica Acta* 141, 547–566. doi:10.1016/j.gca.2014.06.037
- Wallace, M. E., and Green, D. H. (1988). An Experimental Determination of Primary Carbonatite Magma Composition. *Nature* 335, 343–346. doi:10.1038/335343a0
- Wang, Y., Sakamaki, T., Skinner, L. B., Jing, Z., Yu, T., Kono, Y., et al. (2014). Atomistic Insight into Viscosity and Density of Silicate Melts under Pressure. *Nat. Commun.* 5, 3241. doi:10.1038/ncomms4241
- Webb, S. (1997). Silicate Melts: Relaxation, Rheology, and the Glass Transition. *Rev. Geophys.* 35 (2), 191–218. doi:10.1029/96rg03263
- Wilding, M., Bingham, P. A., Wilson, M., Kono, Y., Drewitt, J. W. E., Brooker, R. A., et al. (2019). CO₃+1 Network Formation in Ultra-High Pressure Carbonate Liquids. *Sci. Rep.* 9, 2–5. doi:10.1038/s41598-019-51306-6
- Wilding, M. C., Wilson, M., Alderman, O. L. G., Benmore, C., Weber, J. K. R., Parise, J. B., et al. (2016). Low-Dimensional Network Formation in Molten Sodium Carbonate. *Sci. Rep.* 6, 24415. doi:10.1038/srep24415
- Wilson, M., Ribeiro, M. C. C., Wilding, M. C., Benmore, C., Weber, J. K. R., Alderman, O., et al. (2018). Structure and Liquid Fragility in Sodium Carbonate. *J. Phys. Chem. A* 122, 1071–1076. doi:10.1021/acs.jpca.7b10712
- Woolley, A. R., and Kjarsgaard, B. A. (2008). *Carbonatite Occurrences of the World: Map and Database. Geological Survey of Canada, Open File Report 5796.* doi:10.4095/225115
- Yaxley, G. M., and Brey, G. P. (2004). Phase Relations of Carbonate-Bearing Eclogite Assemblages from 2.5 to 5.5 GPa: Implications for Petrogenesis of Carbonatites. *Contrib. Mineralogy Petrol.* 146, 606–619. doi:10.1007/s00410-003-0517-3
- Yaxley, G. M., Crawford, A. J., and Green, D. H. (1991). Evidence for Carbonatite Metasomatism in Spinel Peridotite Xenoliths from Western Victoria, Australia. *Earth Planet. Sci. Lett.* 107, 305–317. doi:10.1016/0012-821X(91)90078-V
- Zhang, Y., Otani, A., and Maginn, E. J. (2015). Reliable Viscosity Calculation from Equilibrium Molecular Dynamics Simulations: A Time Decomposition Method. *J. Chem. Theor. Comput.* 11, 3537–3546. doi:10.1021/acs.jctc.5b00351

Conflict of Interest: The authors declare that the research was conducted in the absence of any commercial or financial relationships that could be construed as a potential conflict of interest.

Publisher's Note: All claims expressed in this article are solely those of the authors and do not necessarily represent those of their affiliated organizations, or those of the publisher, the editors and the reviewers. Any product that may be evaluated in this article, or claim that may be made by its manufacturer, is not guaranteed or endorsed by the publisher.

Copyright © 2021 Ritter, Guillot, Sator, Desmaele, Massuyeau and Sanchez-Valle. This is an open-access article distributed under the terms of the Creative Commons Attribution License (CC BY). The use, distribution or reproduction in other forums is permitted, provided the original author(s) and the copyright owner(s) are credited and that the original publication in this journal is cited, in accordance with accepted academic practice. No use, distribution or reproduction is permitted which does not comply with these terms.